

SWTCC 2018

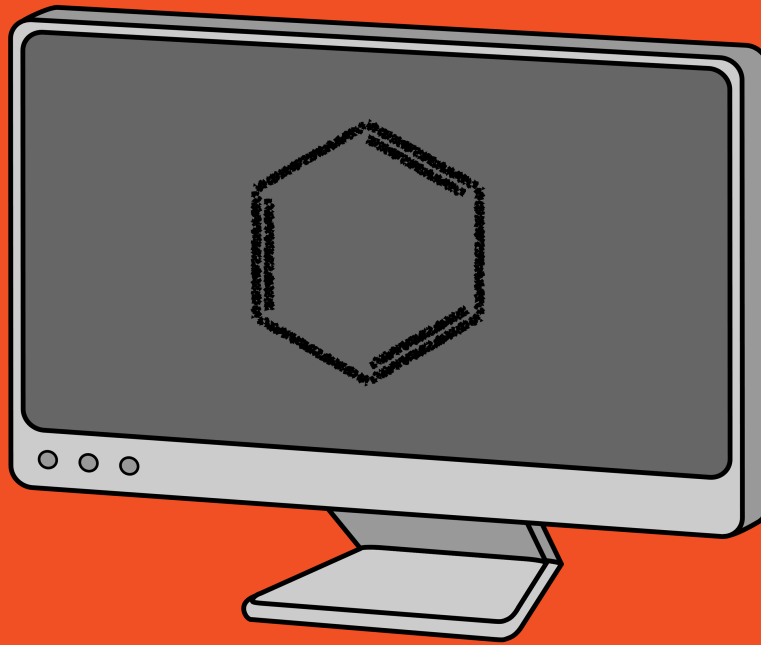
**SOUTHWEST THEORETICAL &
COMPUTATIONAL CHEMISTRY 2018**

**THE UNIVERSITY OF TEXAS RIO GRANDE VALLEY
EDINBURG AND BROWNSVILLE CAMPUSES
OCTOBER 19TH-21ST, 2018**

swtcc@utrgv.edu | <http://www.utrgv.edu/swtcc> | **@SWTCCHEM**

Contents

1	MEETING INFORMATION	3
1.1	Organizers	4
1.2	About UTRGV	4
1.3	Meeting Location & Rooms	4
1.4	Getting to Campus & Parking	5
1.5	Conference Hotels	5
1.6	Registration Payments	5
1.7	Wireless Access	6
1.8	Participating in SWTCC Virtually	6
1.9	Poster Session	6
1.10	Banquet	6
1.11	Weather Advisory	7
2	TECHNICAL PROGRAM	8
2.1	FRIDAY EVENING—Shervin Fatehi, Chair	9
2.2	SATURDAY MORNING—Bill Poirier, Chair	9
2.3	SATURDAY AFTERNOON—Eric Bittner, Chair	10
2.4	SUNDAY MORNING—Yihan Shao, Chair	10
2.5	About the Plenary Lecturers	11
2.5.1	Jiří Vaníček	11
2.5.2	Dmitrii Makarov	11
3	ABSTRACTS OF TALKS	12
4	POSTER ABSTRACTS	29
5	LIST OF PARTICIPANTS	36
6	CAMPUS MAPS	38



SWTCC 2018

MEETING INFORMATION

1.1 Organizers

The principal organizer for SWTCC 2018 is Dr. Shervin Fatehi of the University of Texas Rio Grande Valley, who has benefited immensely from the guidance of immediate past co-organizer Dr. Bill Poirier of Texas Tech. If you have any questions or concerns, you may contact Dr. Fatehi (shervin.fatehi@utrgv.edu or (510) 292-5446). Also assisting with SWTCC are UTRGV Chemistry's department assistant Mr. Andres Sanchez (andres.sanchez02@utrgv.edu or (956) 665-3371) and Dr. Fatehi's research students, Ms. Catherine Clark and Mr. Daniel Piñon.

1.2 About UTRGV

“The University of Texas Rio Grande Valley (UTRGV) was created by the Texas Legislature in 2013 as the first major public university of the 21st century in Texas. This transformative initiative provided the opportunity to expand educational opportunities in the Rio Grande Valley, including a new School of Medicine, and made it possible for residents of the region to benefit from the Permanent University Fund — a public endowment contributing support to the University of Texas System and other institutions.

“UTRGV has campuses and off-campus research and teaching sites throughout the Rio Grande Valley including in Boca Chica Beach, Brownsville (formerly The University of Texas at Brownsville campus), Edinburg (formerly The University of Texas-Pan American campus), Harlingen, McAllen, Port Isabel, Rio Grande City, and South Padre Island. UTRGV, a comprehensive academic institution, enrolled its first class in the fall of 2015, and the School of Medicine welcomed its first class in the summer of 2016.”

The above description is taken from <https://www.utrgv.edu/en-us/about-utrgv/history>. As of Fall 2018, the UTRGV Department of Chemistry consists of 22 tenure-track and tenured-faculty, spread across all of the major disciplines of chemistry; 16 lecturers; and 6 administrative and technical staff. We offer BS and MS degrees, including an undergraduate degree with UTeach certification, and are funded at the departmental level by the Howard Hughes Medical Institute, the Welch Foundation, and the Elliott Chemical Society.

1.3 Meeting Location & Rooms

SWTCC will be held primarily in the Mathematics & General Classrooms (MAGC) Building on the Edinburg campus of UTRGV (1201 West University Drive), with a simulcast to the Brownsville campus (1 West University Boulevard). We encourage you to attend the conference in Edinburg, where talks will be given. Relevant room numbers are:

Edinburg lecture hall MAGC 1.302

Edinburg poster session MAGC 1th floor lobby

Brownsville lecture hall Main Building 1.220

Maps of the Edinburg and Brownsville campuses of UTRGV are provided in Section 6 of this program, starting on p. 38.

1.4 Getting to Campus & Parking

Those of you who are driving to the Valley will likely want to commute from your hotel to the Edinburg campus of UTRGV. Permit enforcement is suspended on campus over the weekend, so parking will only be an issue on the afternoon of October 19th. We expect to receive 15 visitor permits around 1 PM; you may request one to print and display in your vehicle, or you can obtain one from us when you arrive on campus. The visitor permit should allow you to park in any Zone 3 (faculty/staff) parking space; the Zone 3 parking lots most convenient to the MAGC building (#40) are Lots E12 and E14, which are boxed in yellow on the detail map below:



Those registrants who will not have a car are encouraged to carpool with those who do when possible, or to use hotel shuttles where they are offered. In the event that neither of these options is available to you, both Lyft and Uber operate in the Rio Grande Valley and are fairly reliable; a variety of conventional taxi services can be found through Google or Yelp searches, but they generally take longer to pick-up and drop-off.

1.5 Conference Hotels

Comprehensive hotel information—including times for shuttles to the Edinburg campus of UTRGV, where such services are available—may be found on the Travel & Hotels page of the SWTCC website. Should you have any problems with your reservation, please contact the organizers.

1.6 Registration Payments

Registration fees and deadlines are described in detail on the Registration page of the SWTCC website. The organizers will accept checks throughout the conference, but we recommend that you register with the UTRGV ePay service and remit payment through our event page:

https://webapps.utrgv.edu/it/em/index.cfm?event=Public.View.Courses&Event_id=1402

We will be available to provide assistance with ePay at the beginning of the Friday evening and Saturday morning sessions.

1.7 Wireless Access

30 guest accounts for UTRGV's computing resources have been created for SWTCC participants. Each account provides access to the podium computer in classrooms, to campus computer labs, and to the eduroam wireless network. (If your home institution uses eduroam, you should be able to log in with your own credentials.) Account information may be obtained from the organizers on request.

1.8 Participating in SWTCC Virtually

Some of you have registered for Virtual SWTCC, while others (such as those who are experiencing travel delays) may wish to attend some talks by teleconference. The conference will be streaming via Zoom, and is accessible during the set meeting times on PC, Mac, Linux, iOS, and Android platforms at the following (clickable) link: <https://zoom.us/j/319641390>. You may wish to join the meeting early so that you can download and install the Zoom client.

If your internet service is unavailable or unreliable, you may also dial into the meeting audio as listed below; please dial the number with an area code nearer to your current location for optimal audio quality.

Land-Line Telephone (669) 900-6833 or (929) 436-2866, with Meeting ID 319 641 390.

iPhone One-Tap Dialing +16699006833,,319641390# or +19294362866,,319641390#

During the Q&A period at the end of each talk, Virtual SWTCC registrants may submit questions directly to the SWTCC Twitter (@SWTCCChem, <https://twitter.com/swtccchem>). The account will be monitored by the organizers during these periods, and questions will be referred to the session chair.

1.9 Poster Session

The SWTCC poster session will take place in the lobby of the Mathematics & General Classrooms building at 2:30 PM on October 20th. 30" × 40" poster boards will be placed on easels in the lobby in the morning to provide an opportunity for the presenters to post their work. Binder clips will be provided to secure the posters to the boards. Please plan to remove your poster before the end of the day on Saturday!

1.10 Banquet

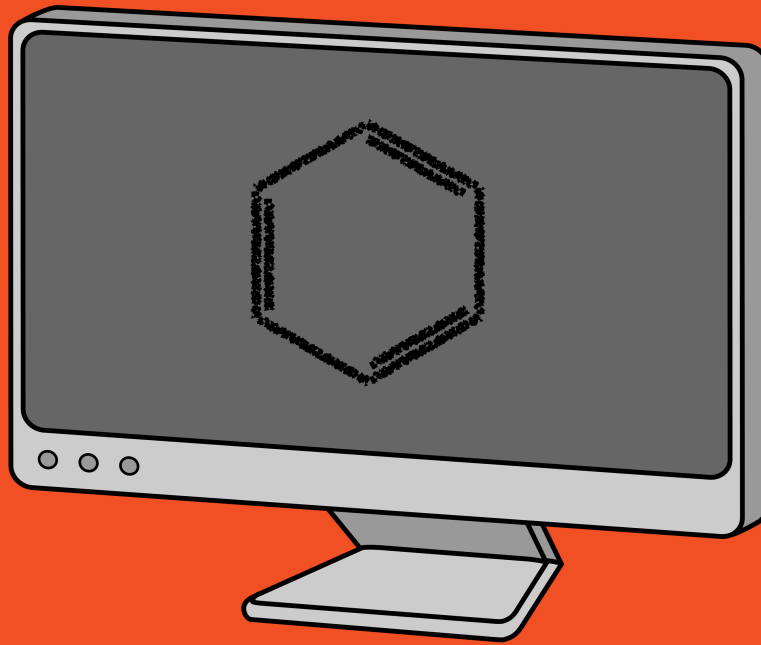
The conference banquet and steering meeting for SWTCC 2019 will be held at SALT New American Table (<https://saltnewamericantable.com>) at 8 PM on the evening of October 20th. Included with your registration/banquet ticket are a salad (spinach or heirloom tomato); entrée (filet mignon, duck breast, ahi tuna, or seasonal vegetarian/vegan bowl); dessert (baked Alaska or chocolate mousse tart); and two non-alcoholic beverages. Should you wish to order beer, wine, or spirits, you will need to pay for those drinks on a separate check.

SALT is located at 210 North Main Street in McAllen, catty-corner to the Casa de Palmas, one of our conference hotels. In addition to street parking, there is a public parking lot just around the corner at the City of McAllen's Archer Park. We encourage registrants who are driving to the Valley to carpool to the banquet with those registrants who do not have vehicles; directions for the most straightforward route from the Edinburg campus of UTRGV are available at <https://goo.gl/maps/qzYsJsXrh6T2>.

Please note: SALT has advised us that we are nearing the limit of banqueters that can be accommodated. If you have not already confirmed with the organizers that you will be attending or bringing a guest by indicating such on the registration form or in your ePay, please contact us to do so.

1.11 Weather Advisory

Several bands of rainstorms have been moving through Texas over the last week, and unseasonably cold temperatures have accompanied the rain. Unfortunately, both the rain and the (relative) chill are expected to continue throughout our conference weekend, with daytime temperatures in the 70s and upper 80s and nighttime temperatures in the upper 60s. While we were expecting typical October weather—sunny days in the 80s and 90s—we hope that you will return to the Valley to enjoy our mild winters and bracingly hot summers... and to collaborate on some chemistry!



SWTCC 2018

TECHNICAL PROGRAM

2.1 FRIDAY EVENING—Shervin Fatehi, Chair

4:30p Registration/ePay assistance (Shervin Fatehi, UTRGV).

5:00p Welcome. (Mohammed Farooqui {Dean, UTRGV College of Sciences}
Yuanbing Mao {Chair, UTRGV Department of Chemistry})

5:20p Introductory remarks (Shervin Fatehi, UTRGV).

5:30p 1. Cryo-electron microscopy extended into the quantum realms of photosynthetic energy transfer processes (Andreas Holzenburg, UTRGV).

6:10p 2. Mechanistic studies on palladium(0)-catalyzed cyclization of diketooesters (Tulay Atesin, UTRGV).

6:50p 3. Computational modeling of substituent effect on the frontier orbitals of conjugated molecules (Yihan Shao, Oklahoma).

2.2 SATURDAY MORNING—Bill Poirier, Chair

8:00a Registration/ePay assistance (Shervin Fatehi, UTRGV).

8:30a 4. Probing coherence dynamics with two-dimensional photoexcitation spectroscopy. (Hao Li, Houston).

9:10a 5. Mapping polaronic distortions across the metal-insulator transition of nanoscale β' -Cu_xV₂O₅ (Abhishek Parija, Texas A&M).

9:50a Break.

10:20a 6. Theory of nonlinear spectroscopy with entangled quantum photons (Eric Bittner, Houston).

11:00a 7. Plenary Lecture: On-the-fly ab initio semiclassical approach to vibrationally resolved electronic spectra (Jiří Vaníček, EPFL).

2.3 SATURDAY AFTERNOON—Eric Bittner, Chair

2:30p Poster session.

3:30p 8. Exploring the reliability of a homology model of GPR119 receptor to predict the EC_{50} s of a set of agonist compounds (Evangelia Kotsikorou, UTRGV).

4:10p 9. Sulfur Mass Independent Fractionation (S-MIF): How quantum dynamics is answering fundamental questions about the origins of life (Bill Poirier, Texas Tech).

4:50p Break.

5:20p 10. Calculation of high-level *ab initio* rate constants for key neutral–neutral reactions in low-temperature Titan conditions (Shiblee Barua, NASA Goddard).

6:00p 11. Plenary Lecture: Barrier crossing dynamics from single-molecule trajectories (Dmitrii Makarov, UT Austin).

8:00p SWTCC Banquet at SALT New American Table.

2.4 SUNDAY MORNING—Yihan Shao, Chair

8:30a 12. MO_2 ($M = Si, Ge, Ti$) cristobalite-rutile transformations (Shariq Haseen, UT Arlington).

9:10a 13. Better optical performance of $La_2Hf_2O_7$ over $La_2Zr_2O_7$: Experimental evidence supported by theoretical calculations (Santosh Gupta, UTRGV and Bhabha Atomic Research Centre).

9:50a Break.

10:20a 14. Finite-size corrections to the free energy of boundaryless Coulomb systems (Jeff Thompson, UT Austin).

11:00a 15. Application of data science technologies to chemical and physics computations (Jonathan Jerke, Texas Tech).

11:40a 16. Solution of mathematical model for gas solubility using fractional-order Bhatti polynomials (Muhammad Bhatti, UTRGV).

12:20p Concluding remarks (Shervin Fatehi, UTRGV).

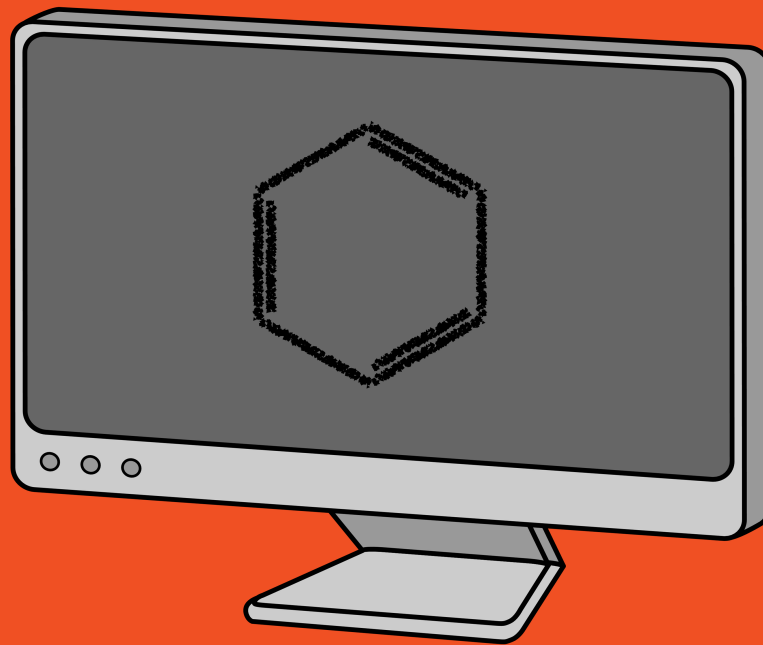
2.5 About the Plenary Lecturers

2.5.1 Jiří Vaníček

Jiří Vaníček earned both his bachelor's degree and doctorate in theoretical physics at Harvard, working on uniform semiclassical approximations and quantum chaos under the supervision of Eric Heller. From 2003 to 2005, he held postdoctoral positions at the Mathematical Sciences Research Institute, Berkeley, and in William Miller's group at the University of California in Berkeley, where he worked on the quantum instanton approximation for kinetic isotope effects. After that, he spent two years as a fellow at the Institute for Advanced Study in Princeton, applying methods of statistical physics to predict genes regulated by microRNAs in herpesviruses. In 2007, Jiří Vaníček joined the faculty of École Polytechnique Fédérale de Lausanne (EPFL), where he is an associate professor of theoretical physical chemistry. His research interests include the development of efficient methods for on-the-fly ab initio semiclassical and nonadiabatic quantum dynamics, with applications in electronic spectroscopy, and for the Feynman path integral approach to quantum statistical mechanics, in order to study quantum effects on thermodynamic properties and rate constants.

2.5.2 Dmitrii Makarov

Dmitrii Makarov earned a bachelor's degree in physics from the Moscow Institute of Physics and Technology, with a doctorate in theoretical physics from the Institute of Chemical Physics (Chernogolovka) following two years later. From 1993–2000, he held postdoctoral positions at the University of Illinois at Urbana–Champaign and the University of California, Santa Barbara. In 2001, he assumed an assistant professorship in the Department of Chemistry and Biochemistry at the University of Texas at Austin, where he is now full professor, associate chair, and director of undergraduate education. His research achievements relating to chemical dynamics and the requisite theories for describing and interpreting single-molecule experimental techniques have earned him several awards—including an NSF CAREER award in 2004 and the 2012 Moncrief Grand Challenge Faculty Award—and have resulted in the publication of two books and 125 papers.



SWTCC 2018

ABSTRACTS OF TALKS

Cryo-electron microscopy extended into the quantum realms of photosynthetic energy transfer processes

Holzenburg, A.¹ and Perez, L.²

¹ UTRGV, United States, ² Texas A&M University, United States

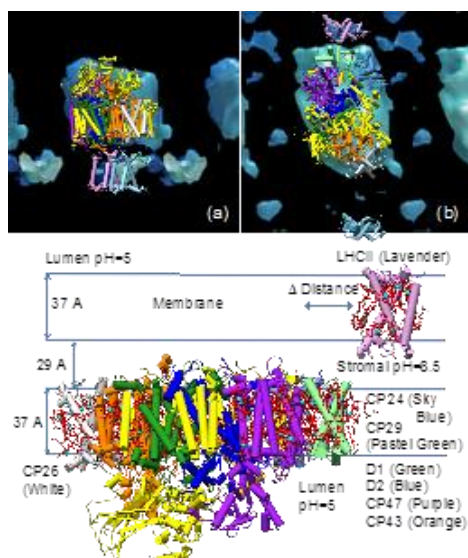


Figure 1. Crystal structures of PSII core (2AXT), LHCII (1RW7), and CP29 (3PL9) fitted into the *in situ* electron tomographic data viewed normal (a) and perpendicular (b) to the thylakoid membrane plane. Below, PSII atomistic model based on X-ray and cryo-EM data.

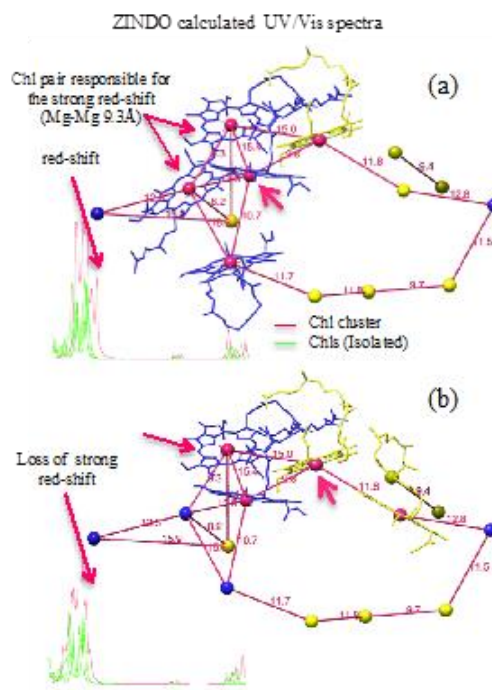


Figure 2. ZINDO calculated UV/Vis spectra for two possible Chl clusters in LHCII: (a) Chl cluster showing a red-shift. (b) Chl cluster without a red-shift. Blue-Chlb, Yellow-Chla, Magenta - Mg atoms of Chl included in the calculation.

Quantum

phenomena are intrinsic to many phenomena in living systems such as birds and butterflies detecting the Earth's magnetic field, olfactory reception, ion channel-based concerted firing of action potentials culminating in conscious thoughts, quantum-tunneled electron travel in the respiratory chain, or the highly efficient quantum coherence-enabled energy-transfer processes employed by photosynthetic organisms^[1]. With regards to the latter, checking the truth of the underlying principles is challenging as the experimental measurements employed may perturb a quantum system into a classical one^[2]. This has, for instance, been a concern with 2DES experiments employing ultrashort broadband laser pulses when probing the quantum processes of photosynthesis^[3]. Here we propose to uncover the foundations of photosynthetic energy transfer as a role model for other biological quantum systems using an approach that extends experimental data into those realms where the use of a non-perturbing approach is critically required. To this end, this project uses quantum chemical calculations to three-dimensionally map the patterns of quantum and non-quantum effects observed in the highly effective energy transfer process of photosynthesis. Atomistic details have been analyzed in the context of an *in situ* assembly as observed in higher plant thylakoid membranes in leaves of plants grown under controlled light regimes. There is a large body of structural data available for the individual components (X-ray crystallography) of the major photosynthetic complex photosystem II [PSII] and one data set for unperturbed, *in situ* PSII (electron tomography) that includes the 8 transmembrane subunits D1, D2, CP24, CP26, CP29, CP43, CP47, and LHCII. Combining X-ray and electron tomographic data into an atomistic model as a starting point (Fig. 1), this proposal uses both quantum and classical chemical calculations to unravel the energy transfer patterns within the confinement of a single PSII component (**intra-subunit**) and then across the subunit boundaries (**inter-subunit**) to cover the entire complex.

Mechanistic Studies on Palladium(0)-Catalyzed Cyclization of Diketoesters

Tülay Ateşin, Department of Chemistry, The University of Texas Rio Grande Valley

Plausible mechanisms of Pd(0)-catalyzed cyclization of diketoesters were modeled using density functional theory calculations. Comparison of the reaction mechanisms of uncatalyzed and Pd(0)-catalyzed cyclizations revealed the vital role of the Pd(0)-catalyst. Both reactions favor a stepwise mechanism involving a proton transfer followed by carbon–carbon bond formation over either the reverse order or a concerted mechanism. The key step for the Pd(0)-catalyzed reaction is the formation of a relatively stable intermediate, an η^3 -allyl Pd(II) complex, in the lowest energy pathway. Our proposed mechanism is consistent with a Pd(0)-catalyzed intramolecular allylic alkylation reaction, previously referred to as “Nazarov-type” reactions. It is worth noting that, in contrast to many allylic alkylations, the Pd(0)-catalyzed cyclization does not require any additional reagents or an activated leaving group to form an η^3 -allyl Pd(II) complex; thus, the α -hydroxycyclopentenone is produced from diketoesters with no waste. Furthermore, the asymmetric version of this reaction is the first known example of the use of an allylic alkylation reaction for the synthesis of a chiral cyclopentenone unit.

Computational Modeling of Substituent Effect on the Frontier Orbitals of Conjugated Molecules

Yihan Shao

Department of Chemistry, University of Oklahoma, Norman, OK 73072

In the design of fluorescence and bioluminescence probes, it is common to attach electron-donating groups (EDG) and electron-withdrawing groups (EWG) to a fluorophore to adjust its frontier orbital energies and thus the absorption/emission wavelengths. To help understand such substituent effects, we will present a new procedure for analyzing the interactions between fluorophore orbitals and substituent orbitals (Chem. Sci. 2018, 10.1039/C8SC02990C). Using prodan and oxyluciferin as examples, we will show different effects, especially permanent electrostatics and orbital mixing, can play key roles in the modulation of the fluorophore frontier orbitals.

Probing coherence dynamics with two-dimensional photoexcitation spectroscopy

Hao Li, Eleonora Vella, Pascal Grégoire, Carlos Silva, and Eric R. Bittner

Various techniques of 2D photoexcitation spectroscopy have been developed recently and form a powerful tool set to study excited-state dynamics by detecting nonlinear optical signals based upon particular excited-state populations. We here report a theoretical description that interprets the experimental result of 2D photocurrent spectroscopy probing the ultrafast coherent decay of instantaneous photocarriers into polaron states as free-charge precursor in polymer:fullerene based solar cells. We also propose a novel and valuable technique of 2D spectroscopy relied on the quasi-steady-state photoinduced absorption measurement of a long-lived nonlinear population such as metastable polaronic species in bulk heterojunction solar cells.

Mapping polaronic distortions across the metal-insulator transition of nanoscale β' - $\text{Cu}_x\text{V}_2\text{O}_5$

Abhishek Parija,¹ Justin L. Andrews,¹ Joseph V. Handy,¹ and Sarbajit Banerjee¹

¹Department of Chemistry and Department of Material Science and Engineering, Texas A&M University, College Station, TX 77845-3012 (USA)

Email: abhishek.parija@chem.tamu.edu

Transition metal oxides span a vast range of electrical conductivity and include examples of insulators, semiconductors, and metals. Single materials capable of abruptly and cleanly transitioning from insulating to metallic states are exceedingly rare and of great interest for device applications such as Mott field-effect transistors, electro/thermochromic coatings, and memristors. Ternary vanadium oxide bronzes ($\text{M}_x\text{V}_2\text{O}_5$) are a singularly unique class of oxides that exist for a large number of known metal intercalants, M (monovalent and divalent main-group and transition metal cations), and crystallize in a large number of 1D, 2D, and 3D structures.¹ This class of materials also exhibits a variety of sharply nonlinear electronic phenomena including charge and spin density waves, metal-insulator transitions, spin-gap transitions, and superconductivity, arising in part from the rich redox chemistry of vanadium and the ability to readily localize/delocalize charge density. We have previously reported that β' - $\text{Cu}_x\text{V}_2\text{O}_5$ exhibits a metal-insulator transition around 300 K, but have observed that the metal-insulator transition in single nanowires is extremely sensitive to copper stoichiometry, x (β' - $\text{Cu}_x\text{V}_2\text{O}_5$).² The β/β' phase is a pseudo 1D tunnel structure in which the metal cation, in this case, Cu (I) resides within the tunnel and partially reduces specific V^{5+} sites in the V_2O_5 framework to V^{4+} , resulting in charge ordered networks. First-principles density functional theory calculations, photoemission spectroscopy, and single crystal diffraction have been used to probe the mechanistic underpinnings for the metal-insulator transition. We have predicted that the melting of this polaronic state because of subtle perturbations in the position of the copper ions results in the delocalization of the electrons in the charge ordered network, ultimately manifesting in metallic behavior. Insights into the structural and electronic properties underpinning this transition obtained during this study will allow for rational tuning of transition temperature and magnitude (by changing x) and help to establish the structure-function relationship in this material.

References: [1] Marley, P. M.; Abtey, T. a.; Farley, K. E.; Horrocks, G. a.; Dennis, R. V.; Zhang, P.; Banerjee, S. Emptying and Filling a Tunnel Bronze. *Chem. Sci.* **2015**, 6 (3), 1712–1718.

[2] Patridge, C. J.; Wu, T.-L.; Sambandamurthy, G.; Banerjee, S. Colossal above-Room-Temperature Metal-Insulator Switching of a Wadsley-Type Tunnel Bronze. *Chem. Commun.* **2011**, 47 (15), 4484–4486.

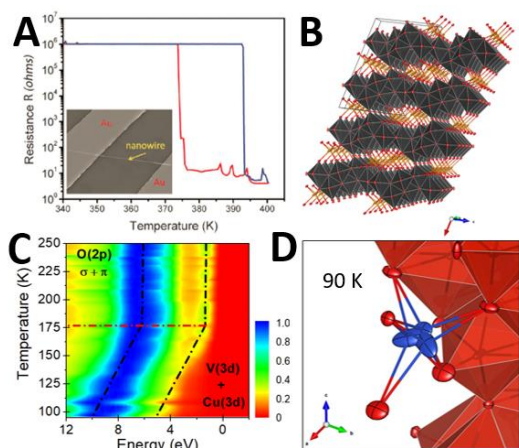


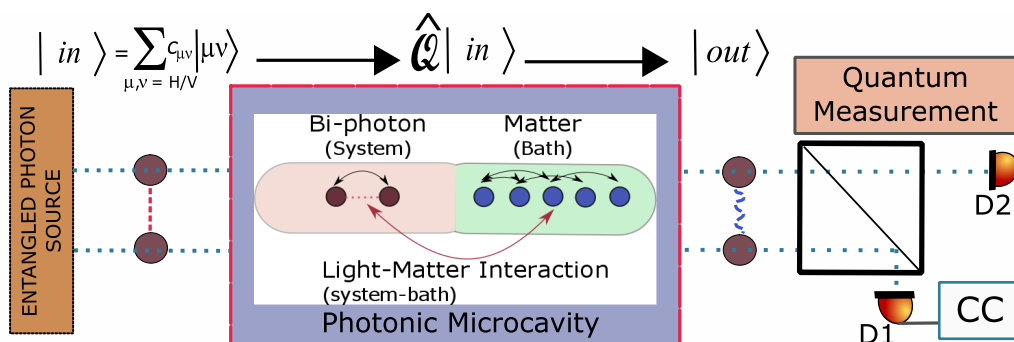
Figure 1. (A) Single-wire electrical transport measurement of resistance versus temperature showing a large discontinuous jump in R and transition to a metallic state near 380 K. Magnified SEM image in the inset shows a typical single-nanowire device; (B) The crystal structure of β' - $\text{Cu}_x\text{V}_2\text{O}_5$; (C) Angle integrated photoemission spectra of β' - $\text{Cu}_{0.4}\text{V}_2\text{O}_5$ depicting the evolution of the valence band with increase in temperature; (D) Single crystal X-ray diffraction structure of β' - $\text{Cu}_{0.4}\text{V}_2\text{O}_5$ showing the symmetric and non-symmetric sites of intercalated Cu-ion.

Theory of Nonlinear spectroscopy with entangled quantum photons

Hao Li¹, Andrei Piryatinski², Ajay R. S. Kandada³, Carlos Silva³, and Eric R. Bittner¹
¹Department of Chemistry, Univ. of Houston, ²Los Alamos National Laboratory, ³Georgia Tech.

ABSTRACT

Recent theoretical and experiments have explored the use of entangled photons as a spectroscopic probe of material systems. We develop here a theoretical description for entropy production in the scattering of an entangled biphoton state within an optical cavity. I will discuss our recent theoretical advances that explore how photon-photon entanglement provides a robust and sensitive probe of many-body correlations in cavity QED. By carefully tuning the cavity, one can “dial” in the entanglement of the output state, thereby providing a means for an addressable universal quantum logic gate.

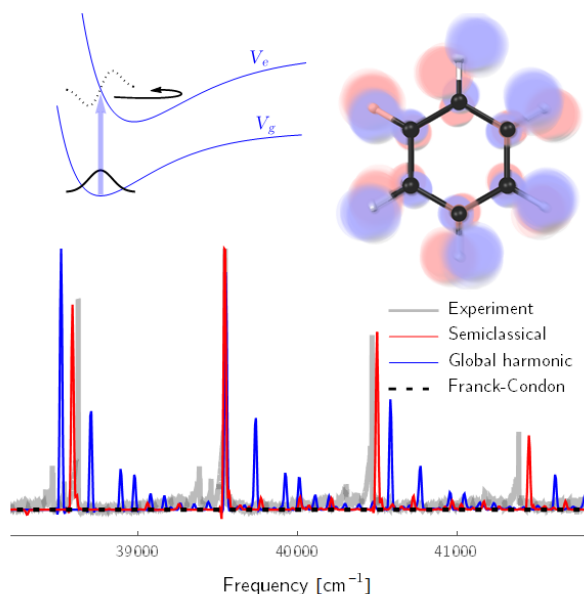


On-the-fly ab initio semiclassical approach to vibrationally resolved electronic spectra

Jiří Vaníček

Vibrationally resolved electronic spectra pose a challenge to the theory of chemical dynamics because an accurate description of such spectra depends both on the quality of the electronic potential energy surfaces and on the inclusion of nuclear quantum effects. On-the-fly ab initio semiclassical dynamics address both issues simultaneously. I will present an on-the-fly ab initio implementation [1,2] of the thawed Gaussian approximation [3], a very simple semiclassical method, which, nevertheless, goes far beyond the standard approaches by including vibrational mode distortion, Duschinsky rotation, and anharmonicity. I will demonstrate the utility of the ab initio thawed Gaussian approximation on several examples of vibrationally resolved electronic absorption, emission, and photoelectron spectra of both floppy (ammonia [2]) and large molecules (oligothiophenes with up to 105 vibrational degrees of freedom [1]). To describe electronic spectra beyond the Condon approximation, we have also implemented two extensions [4,5] by considering the Herzberg-Teller contribution due to the dependence of the electronic transition dipole moment on nuclear coordinates; the electronically forbidden transition in benzene provides a beautiful extreme example because the Condon approximation yields a “zero” spectrum (see figure). Finally, I will mention how the ab initio thawed Gaussian approximation can be applied to ultrafast spectroscopy and how the information contained in a single semiclassical trajectory can be used to interpret spectra of polyatomic molecules and also to generate reduced dimensionality models accessible to exact quantum dynamics [1].

- [1] M. Wehrle, M. Šulc, and J. Vaníček, *J. Chem. Phys.* **2014**, *140*, 244114.
[2] M. Wehrle, S. Oberli, and J. Vaníček, *J. Phys. Chem. A* **2015**, *119*, 5685.
[3] E. J. Heller, *J. Chem. Phys.* **1975**, *62*, 1544.
[4] A. Patoz, T. Begušić, and J. Vaníček, *J. Phys. Chem. Lett.* **2018**, *9*, 2367.
[5] T. Begušić, A. Patoz, M. Šulc, and J. Vaníček, *Chem. Phys.*, **2018**,
<https://doi.org/10.1016/j.chemphys.2018.08.003>.



Exploring the reliability of a homology model of GPR119 receptor to predict the EC₅₀s of a set of agonist compounds

by Evangelia Kotsikorou

GPR119 receptor is a target for type 2 diabetes therapies. Many different compounds have been synthesized to date in hopes of discovering an orally available and effective therapy for T2D. Crystal structures assist in the development of potent ligands for the receptor, but there is no crystal structure of this receptor available today. In the absence of a crystal structure, we constructed a homology model of the receptor that can be used to identify and develop new potent compounds. To test the reliability of the homology model, we conducted a blind computational study to evaluate the relative potency of a set of compounds. Docking studies followed by analysis of the interactions between the docked ligands and the receptor shed light on the types of interactions these compounds have with the receptor, the magnitude of these interactions and the importance of specific amino acids of the binding pocket in ligand binding. The analysis showed that the homology model estimated correctly the energy of interaction of these compounds with the receptor. The energy of interaction of a compound correlates with the potency for activating the receptor. The experimental EC₅₀s were in agreement with the predicted potency of the set of compounds, validating the GPR119 receptor homology model and suggesting that it is a valuable tool for predicting compound potencies.

**Sulfur Mass Independent Fractionation (S-MIF):
How quantum dynamics is answering fundamental questions about the origins of life**

Bill Poirier and Praveen Kumar

*Department of Chemistry and Biochemistry, and Department of Physics,
Texas Tech University, PO Box 41061, Lubbock TX 79409-1061
Bill.Poirier@ttu.edu*

Recent years have seen substantial and growing interest in the spectroscopy and dynamics of SO₂, across a broad range of disciplines that includes molecular astrophysics, atmospheric science, and geochemistry. In the latter discipline, this interest stems largely from the unexpected discovery in 2000 that sulfur mass-independent fractionation (S-MIF) signatures in the geological rock record correlate to the “oxygen revolution” that occurred 2.4 billion years ago. As the source of the S-MIF signal is widely presumed to be SO₂ photodissociation in the atmosphere, advancing our understanding of S-MIF in the rock record—and consequently, of the oxygen revolution itself—requires a mechanistic understanding of SO₂ photodissociation in the gas phase that is sufficiently detailed and accurate to account for subtle sulfur isotope effects.

In short, it requires the tools of “exact” quantum dynamics—as was acknowledged by NASA several years ago, after a decade of approximate simulations failed to lead to the desired answers. This, in turn, has led over the past few years to several vigorous and fruitful cross-disciplinary collaborations with chemical quantum dynamicists.

Our contribution within this broad effort is to investigate the isotopic variation of the relevant rovibronic bound states of SO₂, for all four stable sulfur isotopes^{32–34,36S}, in comprehensive and spectroscopically accurate detail. Both the X^1A_1 ground and C^1B_2 excited singlet electronic states are considered, as these are believed to be the most important players in the photodissociation dynamics vis-à-vis the generation of S-MIF. UV photoabsorption is also characterized in accurate detail, making use of a transition dipole surface. New and highly experimentally accurate potential energy surfaces are employed, developed for X^1A_1 , C^1B_2 , and the transition dipole by collaborators M. Alexander and H. Guo. This work, together with time-dependent wavepacket simulations performed by collaborator Guo, and experiments performed by collaborator A. Mullin, is greatly facilitating our understanding of the origin of S-MIF in the Archean rock record.

Support from NASA Astrobiology (NNX13AJ49G-EXO) and the National Science Foundation (CHE-1012662 and CHE-0840493) is gratefully acknowledged, as is the Texas Tech University High Performance Computing Center, and the Texas Advanced Computing Center.

Calculation of high-level *ab initio* rate constants for key neutral–neutral reactions in low-temperature Titan conditions

Shiblee R. Barua^{1,2} (shiblee.barua@nasa.gov), Paul N. Romani¹

¹NASA Goddard Space Flight Center (GSFC), Greenbelt, Maryland USA

²Universities Space Research Association (USRA), Columbia, Maryland USA

The ultimate source of the complex photochemistry in Saturn’s largest moon Titan’s upper atmosphere (70–187K) is its background neutral environment which is composed primarily of N₂ and CH₄. Previous photochemical models show that such complex chemistry is strongly influenced by neutral–neutral reactions. Global sensitivity analyses confirm that the large errors associated with the mole fractions of various compounds in the upper atmosphere of Titan originate mainly from the uncertainties in low-temperature rate constants of “key” neutral–neutral reactions. Unfortunately, accurate experimental rate constants for such low-*T* reactions are difficult, if not impossible, to measure, and the lab data are affected by uncertainties in determining the absolute concentrations of radical species. Currently, the most common theoretical approach involves uncertainty extrapolation technique in which uncertainties in room-temperature rate constants are extrapolated to low-temperature conditions, resulting in large errors in the theoretical low-*T* rate constant data. To solve this existing problem, we are employing the two-transition-state (2TS) model developed by Klippenstein and coworkers to calculate high-level *ab initio* rate-constants for key low-*T* reactions in Titan, and subsequently evaluating the mole fractions using our existing one-dimensional (1D) photochemical model. In particular, we are investigating key reactions that have not yet been studied in the lab, and for which accurate rate coefficients are still unknown. Our highly accurate theoretical rate constants will be made available to the astrochemistry community at large, and our calculated mole fractions will be used to analyze the Composite Infrared Spectrometer (CIRS) observational data which will vastly improve our current knowledge of the atmosphere of Titan.

Table 1: Selected key reactions currently being investigated that are responsible for uncertainties in the mole fraction profiles of major nitrogen species (left-most column) in low-temperature Titan conditions. Each of the key reactions shown here has an absolute Rank Correlation Coefficient value, a quantitative indicator of the sensitivity of model mole fraction profiles on rate constants, greater than the chosen threshold of 0.2 at 100 km or above (right-most column).

Affected Species	Key Reactions	RCC > 0.2
NH ₃	N(⁴ S) + NH ₂ → N ₂ + H + H	(100, 900) km
HNC	N(⁴ S) + ³ CH ₂ → HNC + H	100 km
C ₂ H ₃ CN	CHCN + H → C ₂ N + H ₂	900 km
CH ₂ NH	N(² D) + CH ₄ → NH + CH ₃	900 km
CH ₃ C ₃ N	¹ CH ₂ + CH ₄ → CH ₃ + CH ₃	900 km
CH ₃ C ₃ N	C ₂ N + H → HCN + C	900 km

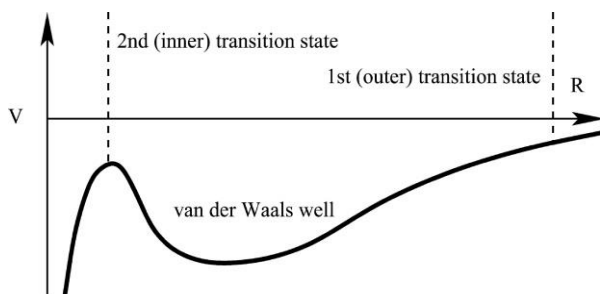


Figure 1. Schematic one-dimensional picture of the potential energy as a function of the reaction coordinate for a neutral–neutral reaction leading to bimolecular products. In its approach, the 2TS model incorporates both the 1st (outer) transition state for barrierless association reaction and the 2nd (inner) transition state for reaction path with a barrier.

Title: Barrier crossing dynamics from single-molecule trajectories

Abstract

The challenge in predicting conformational transition rates from molecular simulations is that transitions are rare events occurring at timescales that are frequently unattainable by brute force simulations. In the experimental realm the challenge is often different: the rate of transitions occurring once per second or once per minute is often straightforward to measure, but the limited time resolution does not allow the experimentalist to say anything about the underlying dynamics that has led to those transitions. It is only recently that single-molecule measurements and atomistic simulations have met halfway, or, more precisely, around a microsecond timescale, which allowed experimentalists to catch (usually bio-)molecules in the act of crossing activation barriers during conformational rearrangements. What can we learn about underlying microscopic dynamics from experimental observations of barrier crossing events given their limited time resolution (microseconds) and given the inherent low dimensionality of the experimental signals? I will describe how exact rate theory can be reformulated in terms experimental observables, such as the mean transition path time and a coarse-grained transition path velocity. Such formulation is conceptually interesting because it looks almost like transition-state theory. More importantly, the transition path velocity has interesting mathematical properties, and it can be measured experimentally even with modest time resolution that is far insufficient for the observation of individual recrossings of the barrier; yet it preserves exact information about such recrossings and can be used to quantify the mean shape of a transition path.

I will further show how a low-time-resolution trajectory $x(t)$ of an experimentally observable reaction coordinate x (aka “experimental signal”) can be used to find out whether or not the underlying dynamics of $x(t)$ is a memoryless Markov process, even if the characteristic memory time of the process is shorter than the time resolution. This result can be used to establish which minimal models (e.g. Kramers theory, Grote-Hynes theory etc.) provide an adequate description for single-molecule signals.

Title: MO_2 (M = Si, Ge, Ti) cristobalite-rutile transformations

Authors: Shariq Haseen, Peter Kroll

We investigate transitions between cristobalite and rutile structures of SiO_2 , GeO_2 , and TiO_2 using density functional theory calculations. The reaction coordinate follows a path that is best described by using a common space group for both structure types. Along the path from cristobalite to rutile, no bonds are broken while the tetrahedrally coordinated cation attains octahedral coordination.

We show that the concerted movement of atoms can be modeled with different degrees of freedom for cations or anions: if anions are collectively following the path, cations can optimize in each step. Conversely, if cations are progressing along the defined path, anions and lattice parameters can freely adjust to each structural change. The two distinct methods yield different activation energies.

In general, we find that activation energies of the forward cristobalite-rutile transformation decrease with increasing pressure. For the reverse transformation from rutile to cristobalite we find that activation energies decrease with decreasing pressure. Thus, we propose that for rutile-type GeO_2 and TiO_2 only moderate negative pressures—comparable to stresses in deposited films—are required to transform the compounds into a cristobalite structure. A hitherto unknown TiO_2 -cristobalite at negative 5 GPa will not only be energetically more favorable than rutile- TiO_2 but can be achieved by an activation of less than 0.3 eV/ TiO_2 .

Better optical performance of $\text{La}_2\text{Hf}_2\text{O}_7$ over $\text{La}_2\text{Zr}_2\text{O}_7$: Experimental evidence supported by theoretical calculations

S. K. Gupta^{1,2}, M. Abdou¹, P.S. Ghosh³, J. P. Zuniga¹, and Y. Mao^{1,4}

¹Department of Chemistry, University of Texas Rio Grande Valley, 1201 West University Drive, Edinburg, Texas 78539, USA

²Radiochemistry Division, Bhabha Atomic Research Centre, Trombay, Mumbai-400085, India

³Materials Science Division, Bhabha Atomic Research Centre, Trombay, Mumbai-400085, India

⁴School of Earth, Environmental, and Marine Sciences, University of Texas Rio Grande Valley, 1201 West University Drive, Edinburg, Texas 78539, USA

Pyrochlore rare earth zirconate and hafnate have been utilized for various applications due to their unique thermophysical, optical and nuclear properties. In this work, we approach through another step to the growing interest in scientific community related to the applications of their nanoparticles in the fields of solid-state lighting and scintillator. Unveiling the optical differences in terms of photoluminescence, quantum efficiency and radioluminescence will open a new gateway for researchers in selecting proper hosts for specific optoelectronic applications. We investigated the effect of changing B site ions (Zr^{4+} vs Hf^{4+}) on the optical properties of undoped $\text{La}_2\text{B}_2\text{O}_7$ NPs and europium doped counterparts. Photoluminescence spectroscopy upon UV irradiation shows violet-blue emission from the $\text{La}_2\text{Hf}_2\text{O}_7$ (LHO) NPs whereas both violet-blue and red emissions could be seen from the $\text{La}_2\text{Zr}_2\text{O}_7$ (LZO) NPs. Density of state (DOS) based on density functional theory (DFT) calculation suggests different energetics of ionized oxygen vacancies in the LHO and LZO NPs. Luminescence spectroscopy of the $\text{La}_2\text{Zr}_2\text{O}_7:\text{Eu}^{3+}$ (LZOE) and $\text{La}_2\text{Hf}_2\text{O}_7:\text{Eu}^{3+}$ (LHOE) NPs demonstrates higher quantum yield, emission output, radioluminescent intensity and luminescence lifetime from the LHOE NPs over the LZOE NPs. The better performance of the LHOE NPs could be attributed to lower surface defects, less non-radiative channels and lower agglomeration. DFT calculations suggest the host to dopant energy transfer is more efficient for the LHOE NPs compared to the LZOE NPs making LHO a better host for Eu^{3+} dopants. Our studies highlight the advantages of LHO over LZO as an advanced material for red phosphor, scintillator and fluoroimmunoassays.

Finite-size corrections to the free energy of boundaryless Coulomb systems

Jeffrey P. Thompson and Isaac C. Sanchez

*McKetta Department of Chemical Engineering
The University of Texas at Austin*

In computer simulations aimed at studying bulk properties, an important question is the extent to which the intensive properties of the simulated system differ from their thermodynamic limiting (bulk) values. This question is particularly relevant for systems with long-range interactions, for instance, model ionic solutions and plasmas in which the particles interact via Coulomb forces. Here we sketch an approach, based on the Debye–Hückel approximation, to estimate finite-size corrections for the sort of Coulomb systems typically studied in simulations—namely, those defined on closed manifolds such as the periodic box $\mathbb{R}^d/\mathbb{Z}^d$ or sphere $\{x \in \mathbb{R}^{d+1} : |x| = 1\}$, where d is the dimensionality of the space. The basic approach follows that of Torres and Téllez [1]; the key difference from that work is that our systems, lacking a boundary, must satisfy the constraint of strict charge neutrality. We recall how to deal with this constraint in the sine-Gordon representation of the Coulomb gas. An interesting consequence of strict neutrality is a phenomenon known in the field of relativistic heavy-ion collisions as “canonical suppression”: in the limit of vanishing interparticle interactions, the densities of charged species in a finite-volume, neutral grand canonical ensemble are suppressed relative to their bulk values. For Coulomb systems in the neutral grand canonical ensemble, this suppression leads to an explicitly volume-dependent Debye screening length.

References

1. A. Torres and G. Téllez, *J. Phys. A: Math. Gen.*, 2004, **37**, 2121–2137; *J. Stat. Phys.*, 2005, **118**, 735–765.

Jonathan Jerke TTU *Presenter and first author*
Eric Bittner UH
Bill Poirier TTU

Application of Data Science technologies to chemical and physics computations

The exact solve of 2, 3, and 4 quantum bodies are possible using my newly released ANDROMEDA code : a few electron plane-wave calculator. Computations can include any mixture of periodic and vacuum boundary conditions in Cartesian coordinates with any 2-body interaction with a Laplace transform. External fields like nuclear charges or harmonic confining fields can also be added. A recently accepted article in Molecular Physics shows the 2-body operators are valid by verification against with Model Hookean theories. Another concurrent article shows exact solutions of Jellium and their comparison with established DFT models of the correlated electron gas. Interesting details of the exchange-correlation functional arise.

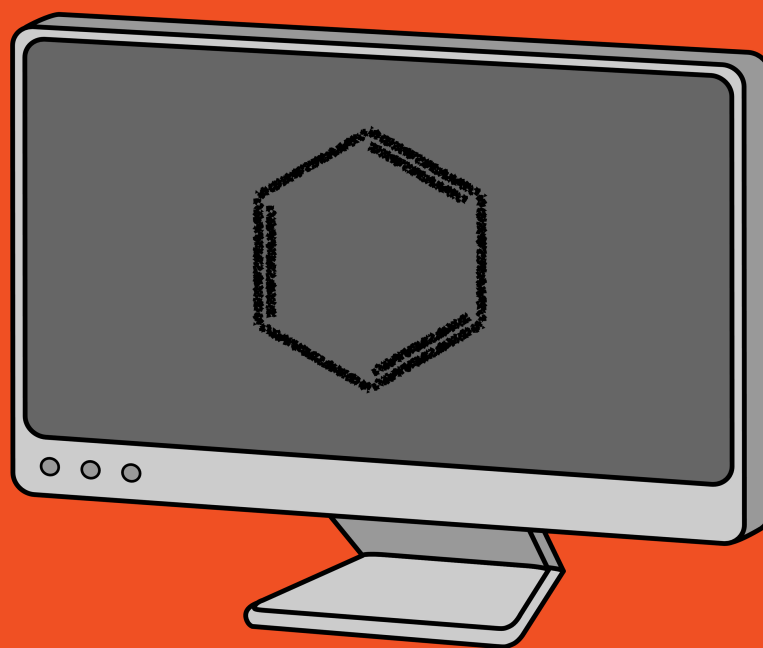
We acknowledge generous support from the Welch Foundation and Texas Tech University

Solution of mathematical model for gas solubility using fractional-order Bhatti Polynomials

Muhammad Bhatti and Armando Herrera
Department of Physics & Astronomy
University of Texas Rio Grande Valley, USA

Abstract:

Solutions of the Mathematical Model for gas solubility in a liquid are attained employing an algorithm based on the generalized Galerkin B-poly basis technique. The algorithm determines a solution of a fractional differential equation in terms of continuous finite number of generalized fractional-order Bhatti Polynomials (B-polys) in a closed interval. The procedure uses Galerkin method to calculate the unknown expansion coefficients for constructing a solution to the fractional-order differential equation. Caputo's fractional derivative is employed to evaluate the derivatives of the fractional B-polys and each term in the differential equation is converted into a matrix problem which is then inverted to construct the solution. The accuracy and efficiency of the B-poly algorithm rely on the size of the basis set as well as the degree of the B-polys used. The fractional-order B-Poly technique has been applied to the Mathematical Model for a gas diffusion in a liquid with gas volume functions $f(t) = 1 - t^{1/2}$ and $1 - t^{3/2}$. The solutions of the model were obtained which converged with a small number of B-polys basis set. In case of the power series solution, the solution did not converge due to alternating terms present in the solution. We used a Pade approximant to the power series solutions to extract the useful information which showed the solutions are convergent and those solutions were compared with the solutions obtained from the B-poly approach. Excellent agreement was found between the solutions. Results will be presented at the conference.



SWTCC 2018

POSTER ABSTRACTS

Correlating Structure and Photo- and Radio-Luminescence of Eu^{3+} Doped $\text{Gd}_2\text{Hf}_2\text{O}_7$ Nanoparticles: Interplay of Experimental and Theory

M. Abdou¹, S. K. Gupta^{1,2}, P.S. Ghosh³, J. P. Zuniga¹, and Y. Mao^{1,4}

¹Department of Chemistry, University of Texas Rio Grande Valley, 1201 West University Drive, Edinburg, Texas 78539, USA

²Radiochemistry Division, Bhabha Atomic Research Centre, Trombay, Mumbai-400085, India

³Materials Science Division, Bhabha Atomic Research Centre, Trombay, Mumbai-400085, India

⁴School of Earth, Environmental, and Marine Sciences, University of Texas Rio Grande Valley, 1201 West University Drive, Edinburg, Texas 78539, USA

Crystal structure has strong influence on the luminescence properties of lanthanide-doped materials. By using Eu^{3+} as a spectroscopic probe, we have investigated the structure and phase transition of $\text{Gd}_2\text{Hf}_2\text{O}_7$ nanoparticles (NPs) induced by thermal annealing. We have studied undoped and Eu^{3+} doped $\text{Gd}_2\text{Hf}_2\text{O}_7$ NPs synthesized at 650 °C (GHOE-650) and two derivatives, which were annealed at 1100 °C (GHOE-1100) and 1300 °C (GHOE-1300). We observed that the undoped and GHOE-650 NPs exist in disordered fluorite phase (DFP) while the GHOE-1100 and GHOE-1300 NPs exist in ordered pyrochlore phase (OPP), and the extent of pyrochlore ordering increases with annealing temperature. The asymmetry ratio of the GHOE-650 NPs was the highest while the quantum yield, luminescence intensity and lifetime values of the GHOE-1300 NPs were the highest. As the structure changes from DFP to OPP, radioluminescence showed tunable color from red to orange. DFT-GGA calculated cohesive energies of ordered pyrochlore and disordered fluorite structures of GHO revealed that ordered pyrochlore structure is stable with respect to the disordered fluorite. Moreover, in the bulk state, the ordered pyrochlore structure is favorable with respect to the disordered fluorite structure. Energies calculated by density functional theory (DFT) support that OPP is the more stable structural form for the GHOE NPs annealed at higher temperature. Moreover our DFT-GGA calculated energetics shows that Eu doping in Hf site is favorable compared to Gd site and the energy difference is 0.74 eV. The distribution of bond lengths and orientation shows that EuO_8 and EuO_6 polyhedra has inversion symmetry when doped in ordered pyrochlore structure and inversion symmetry is absent when doped in disordered fluorite structure. In the density of states of Eu-doped GHOE, Eu-f states contribute solely on the edges of VB and CB in spin-up and spin-down components. The electrons present at the VB edges participate in the photo-excitation. High contribution of Eu-f states at the VB edges makes optical energy transfer of the GHO host to Eu^{3+} dopants favorable.

Allosteric Map of Human Glutathione Synthetase

Brandall L. Ingle¹, Mary E. Anderson², Thomas R. Cundari¹

¹ Department of Chemistry, Center for Advanced Computing and Modeling (CASCaM), University of North Texas, Denton TX 76201

² Department of Chemistry & Biochemistry, Texas Woman's University, Denton TX 76204

Glutathione is a crucial cellular antioxidant; deficiencies are associated with many diseases. Human glutathione synthetase (hGS) is an enzyme responsible for production of glutathione. A homodimer, hGS displays negative cooperativity towards its γ -glutamylcysteine (γ GC) substrate: when γ GC binds in one active site, the second subunit is less likely to catalyze the reaction. Despite more than a century of research, the details of allosteric communication responsible for cooperativity remain a mystery. Allosteric modulation of growing interest in pharmaceuticals, as many drugs target alternate binding sites. As a symmetric enzyme with a relatively small interaction surface, hGS is an ideal model for studying negative cooperativity and allosteric communication. On the basis of experiments and MD simulations, we conclude that the types of amino acids that mediate allosteric communication in hGS differ at binding sites (strongly interacting) and at protein-protein interfaces (weakly interacting) to ensure that the enzyme maintains structure and function, while exhibiting negative cooperativity.

Using wavelets to compute the vibrational states of OCHCO^+

Ankit Pandey and Bill Poirier*

*Department of Chemistry and Biochemistry, Texas Tech University.
2500 Broadway, Lubbock, TX 79409

Abstract: We demonstrate the use of phase space symmetrized Gaussians to calculate the vibrational energy eigenstates of the OCHCO^+ cation. We designed an efficient algorithm to implement various basis set truncation strategies for performing our calculations. A potential energy surface provided by J.Bowman was used, albeit refit to a 6th order anharmonic force field. The latter form is needed by the SwitchBLADE algorithm, which constructs and diagonalizes the vibrational Hamiltonian matrix in order to compute energy eigenstates. Designed by T. Halverson and B. Poirier, SwitchBLADE can switch between the symmetrized Gaussian and the harmonic oscillator basis sets. A theoretical analysis of the underlying concepts, and the functioning of the algorithms used for their application, is presented. The vibrational spectrum of OCHCO^+ is also presented, along with an analysis of the results.

Rovibrational quantum dynamics of the Ne₄ tetramer

Janos Sarka, Corey Petty, Bill Poirier

Department of Chemistry and Biochemistry, Texas Tech University, 1204 Boston Avenue,
Lubbock, Texas, 79409-1061, United States, E-mail: Janos.Sarka@ttu.edu:

The dynamics of rare gas clusters manifest through long-range van der Waals forces that can be challenging to model. Among other challenges (e.g. large masses), such systems are also characterized by equilibrium geometries with large interatomic distances, large anharmonicity, low dissociation threshold energies, and low-lying isomerization barriers leading to fluxional/floppy dynamical behavior.

Among the rare gas clusters, neon clusters present a highly challenging "intermediate" case, between the extremely quantum behavior of helium, and the much more classical behavior of the heavier argon clusters. In particular, from earlier Ne₃ studies [1], there is a clear delineation between the (few) vibrational states that are localized in a single potential well, vs. the fully delocalized states that lie in the "isomerization band." This boundary constitutes a "phase change" or prototypical phase transition, between the "solid" and "liquid" phases of the cluster, which is of interest [2].

In this study, exact quantum dynamics (QD) calculations of the neon tetramer (Ne₄) system were carried out, to determine the bound vibrational and rovibrational states well up into the isomerization band. All Coriolis coupling was treated exactly, in a Jacobi coordinate representation. Calculations were performed using the ScalIT suite of parallel codes [3-5], designed to enable exact QD calculations to be performed on massively parallel computers. The ScalIT codes use a variety of methods (mostly sparse iterative techniques) to enable efficient calculation of quantum states in any desired energy window. In particular, the phase-space optimized discrete variable representation (PSO-DVR) [6] is especially well-suited to systems for which long range interactions (e.g. van der Waals, ion-molecule, etc.) are important.

[1] B. Yang, W. Chen, B. Poirier, *J. Chem. Phys.* **2011**, *135*, 094306.

[2] P. A. Frantsuzov, D. Meluzzi, V. A. Mandelshtam, *Phys. Rev. Lett.* **2006**, *96*, 113401.

[3] C. Petty, B. Poirier, *Appl. Math.* **2010**, *5*, 2756-2763.

[4] W. Chen, B. Poirier, *J. Parallel Dist. Comput.* **2010**, *70*, 779-782.

[5] W. Chen, B. Poirier, *J. Comput. Phys.* **2006**, *219*, 198-209.

[6] B. Poirier, J. C. Light, *J. Chem. Phys.* **2001**, *114*, 6562-6571.

Structure-Activity Relationship of New RGD-Containing Cyclic Octapeptides Against $\alpha_v\beta_3$ Integrin

Aaron Silva¹, Wenwu Xiao², Yan Wang², Hengwei Chang³, Kit S. Lam², Yonghong Zhang¹

¹Department of Chemistry, University of Texas Rio Grande Valley, Edinburg, Texas

²Department of Biochemistry and Molecular Medicine, University of California Davis Cancer Center, Sacramento, California

³C S Bio Company, Menlo Park, California

The $\alpha_v\beta_3$ integrin, a receptor for many extracellular matrix proteins with the RGD-sequence motif, is involved in multiple physiological processes. The integrin is highly expressed on tumor cells, therefore making it a target for cancer therapy and imaging. It has been of great interest to develop an RGD-containing ligand against the $\alpha_v\beta_3$ integrin. A series of RGD-containing cyclic octapeptides (LXW analogs) were previously synthesized, tested in vitro, and screened as the integrin antagonists with different binding affinity (Xiao W 2010; Wang Y, 2015), but the structure-activity relationship still remains to be elucidated. In the current studies, the structures of three representative LXW octapeptides were determined by solution NMR, and then docked to the integrin for complex structure models. The structural comparisons and docking studies showed that the hydrophobicity of the X₇ position of LXW analogs plays a critical role in advancing binding affinity to the integrin. In an effort to develop a more resourceful and efficient method of obtaining protein-ligand docking results, a comparison was made between in vitro examination and computational docking experimentation. A consistency within the results of both methods was found, leading to the continuous optimization and testing of the LXW peptides via computation docking screening. Through our docking results, we have identified several new and potentially improved RGD-containing cyclic octapeptide sequences against the $\alpha_v\beta_3$ integrin.

Reference

- Xiao W, Wang Y, Lau EY, et al. The use of one-bead one-compound combinatorial library technology to discover high-affinity $\alpha_v\beta_3$ integrin and cancer targeting arginine-glycine-aspartic acid ligands with a built-in handle. *Mol Cancer Ther.* 2010 October; 9(10):2714-2723.
- Wang Y, Xiao W, Zhang, et al. Optimization of RGD-containing cyclic peptides against $\alpha_v\beta_3$ integrin. *Mol Cancer Ther.* 2016 Feb;15(2):232-40.

DFT calculation to probe luminescence dynamics in La₂Hf₂O₇:Eu³⁺ nanoparticles

J. P. Zuniga¹, S. K. Gupta^{1,2}, P.S. Ghosh³, M. Abdou¹, and Y. Mao^{1,4}

¹Department of Chemistry, University of Texas Rio Grande Valley, 1201 West University Drive, Edinburg, Texas 78539, USA

²Radiochemistry Division, Bhabha Atomic Research Centre, Trombay, Mumbai-400085, India

³Materials Science Division, Bhabha Atomic Research Centre, Trombay, Mumbai-400085, India

⁴School of Earth, Environmental, and Marine Sciences, University of Texas Rio Grande Valley, 1201 West University Drive, Edinburg, Texas 78539, USA

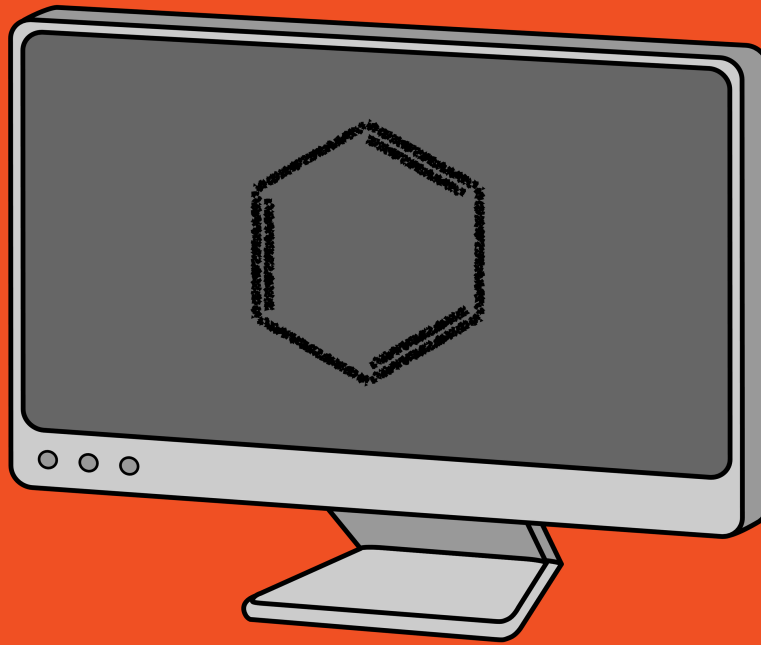
A₂B₂O₇ type pyrochlores have been the focal point of material science research these days because of their various interesting properties such as low thermal conductivity, high dielectric constant, high thermal and structural stability, ability to accommodate dopant ion at both A and B site, and high radiation stability [1, 2]. Undoped La₂Hf₂O₇ (LHO) NPs exhibit multicolor emission (violet blue and red) under near UV excitation [3]. DFT calculations showed charged oxygen defects in the band gap is responsible for photoluminescence in bare NPs. On doping europium in LHO host (LHOE), an efficient host to dopant energy transfer takes place in LHOE which is explained using density of state calculations explained based on DFT calculations. Moreover, our DFT calculated density of state shows Eu doping in LaO₈ site lifts the degeneracy between majority/minority spin components and Eu-f states present at the defect energy levels in both majority and minority spin components. Therefore, origin of most intense red emission in LHOE is mediated through Eu-f states present at charged oxygen defect states in the electronic band-gap and Eu-d states present at valence band. Based on DFT cohesive energy calculations; it is also proposed that europium is energetically more stable at LaO₈ site that is responsible for its highly asymmetric environment in LHO host

References :

[1]. J.P. Zuniga, S.K. Gupta, M. Pokhrel, Y. Mao. *New J. Chem.* 2018, **42**, 9381.

[2] S.K. Gupta, J.P. Zuniga, M. Abdou, Y. Mao. *Inorg. Chem. Front.* 2018. DOI: 10.1039/C8QI00713F

[3] S.K. Gupta, J.P. Zuniga, P.S. Ghosh, M. Abdou, Y. Mao. *Inorg. Chem.* 2018, **57**, 11815.

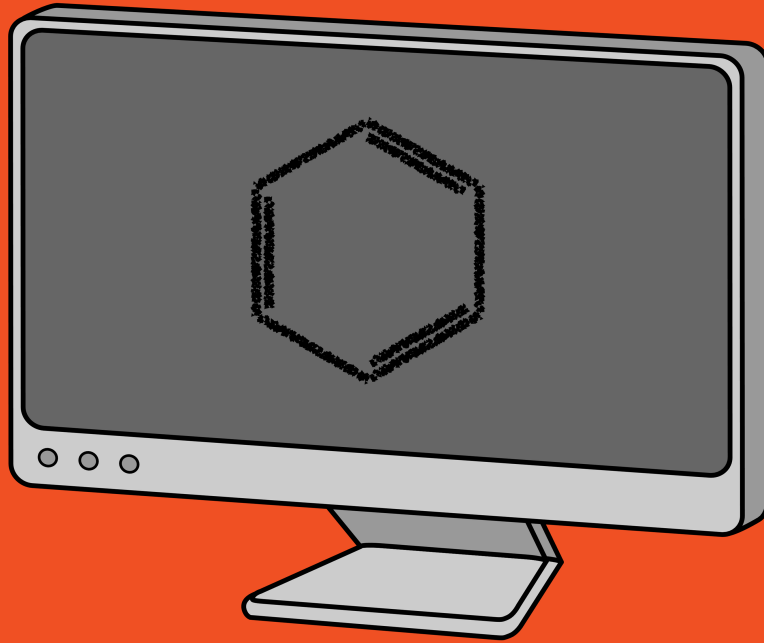


SWTCC 2018

LIST OF PARTICIPANTS

Note: Starred participants are attending virtually.

#	Name	Affiliation
1	Abdou, Maya	The University of Texas Rio Grande Valley
2	Ateşin, Abdurrahman	The University of Texas Rio Grande Valley
3	Ateşin, Tülay	The University of Texas Rio Grande Valley
4	Barua, Shiblee	NASA Goddard Space Flight Center
5	Bhatti, Muhammad	The University of Texas Rio Grande Valley
6	Bittner, Eric	University of Houston
7	Clark, Catherine	The University of Texas Rio Grande Valley
8	Cundari, Thomas	University of North Texas
9	Das, Debojyoti	Texas Tech University
10	Farooqui, Mohammed	The University of Texas Rio Grande Valley
11	Fatehi, Shervin	The University of Texas Rio Grande Valley
12	Gonzalez, Reymundo	The University of Texas Rio Grande Valley
13	Gupta, Santosh	The University of Texas Rio Grande Valley Bhabha Atomic Research Centre
14	Haseen, Shariq	The University of Texas at Arlington
15	Holzenburg, Andreas	The University of Texas Rio Grande Valley
16	Janesko, Benjamin*	Texas Christian University
17	Jayee, Bhumika	Texas Tech University
18	Jerke, Jonathan	Texas Tech University
19	Kotsikorou, Evangelia	The University of Texas Rio Grande Valley
20	Li, Hao	University of Houston
21	Makarov, Dmitrii	The University of Texas at Austin
22	Mao, Yuanbing	The University of Texas Rio Grande Valley
23	Pandey, Ankit	Texas Tech University
24	Parija, Abhishek	Texas A&M University
25	Piñon, Daniel	The University of Texas Rio Grande Valley
26	Poirier, Bill	Texas Tech University
27	Ranathunga, Dineli*	The University of Texas at Dallas
28	Rivera, Diego	The University of Texas Rio Grande Valley
29	Rodriguez Vargas, Oscar	The University of Texas Rio Grande Valley
30	Sarka, Janos	Texas Tech University
31	Serrato, Agapito	Texas State Technical College Harlingen
32	Shao, Yihan	University of Oklahoma
33	Silva, Aaron	The University of Texas Rio Grande Valley
34	Thompson, Jeff	The University of Texas at Austin
35	Vaníček, Jiří	École Polytechnique Fédérale de Lausanne
36	Zuniga, José	The University of Texas Rio Grande Valley



SWTCC 2018

CAMPUS MAPS

Off Campus Facilities:

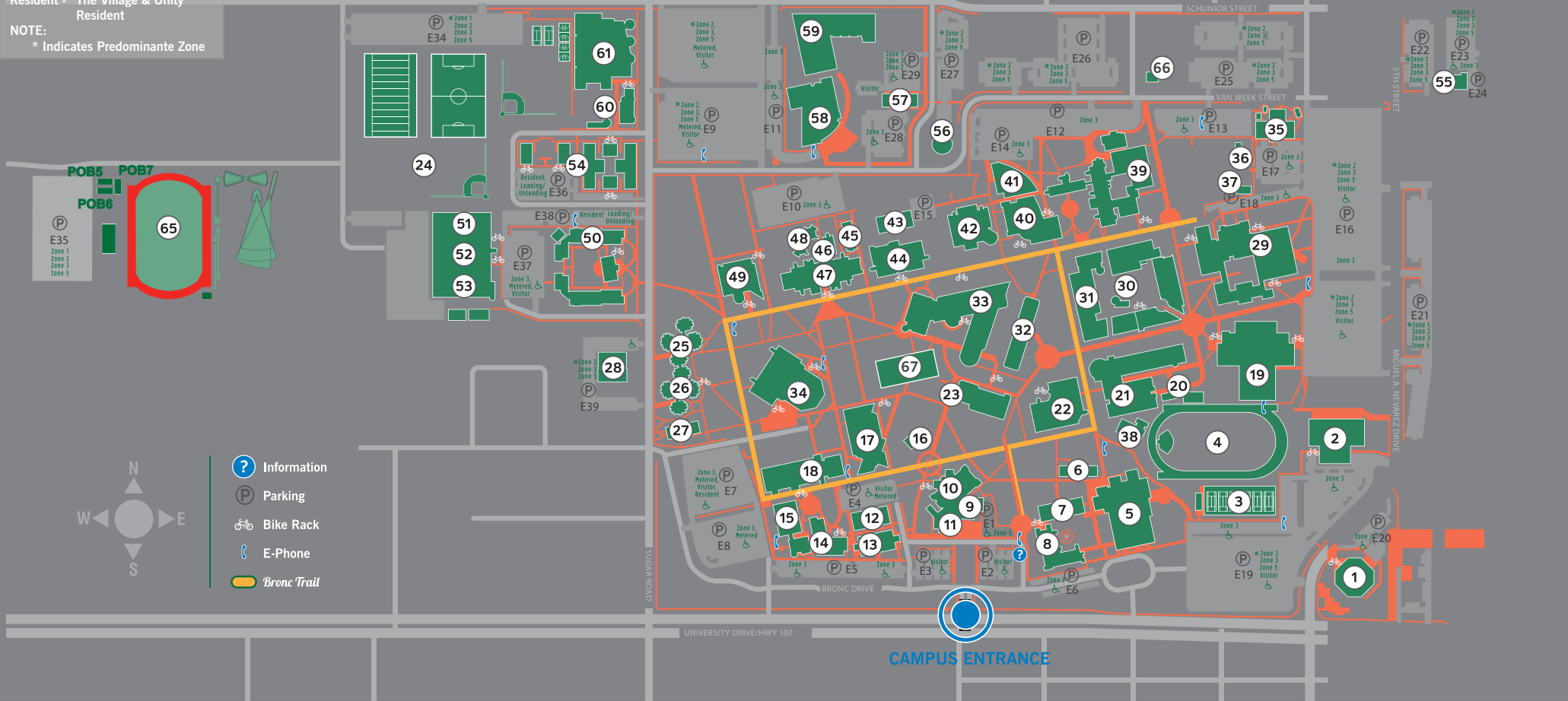
ALUM	-	Alumni Center - Edinburg
ATEC	-	Advance Tooling Engineering Center
CESS	-	Community Engagement & Student Success Bldg.
FNTP	-	Fountain Plaza
JAPC	-	John Austin Pena Clinic
MCTS	-	McAllen Teaching Site
PDSC	-	UT Health Pediatric Specialties Clinic
RHCP	-	UT Health Rheumatology Clinic
USTR	-	Starr County Campus - Rio Grande City
UNFS	-	University Financial Services
VABL	-	Visual Arts Building

UTRGV CAMPUS PARKING

- Zone 1 - Student Parking
- Zone 2 - Student Parking
- Zone 3 - Faculty/Staff Parking
- Zone 5 - Administrator Parking
- Resident - The Village & Unity Resident

NOTE:

* Indicates Predominante Zone



All vehicles parked on campus must be registered with the UTRGV Parking & Transportation Office and must properly display an appropriate permit.

1. ESWOT - Social Work and Occupational Therapy	17. ESTUN - Student Union	33. ELIBR - University Library	46. EHABW - Health Affairs Building West (HSHW - Health Science and Human Services West)	57. ELAMR - Lamar E
2. EITTB - International Trade & Technology	18. EDBCX - Dining & Ballroom Complex	34. ELABS - Liberal Arts Building South (ARHU - Arts and Humanities)	47. EHABW - Health Affairs Building West Classroom A	58. EREBL - Research Education-(School of Medicine) (RAHC - Regional Academic Health Center)
3. ECOXT - Orville Cox Tennis Center	19. EHPE2 - Health & Physical Education II	35. ECDCR - Child Development Center	48. EHABW - Health Affairs Building West Auditorium	59. EMEBL - Medical Education-(School of Medicine)
4. ETRAK - Track & Soccer Field	20. EPOB4 - Engineering Portable	36. EARGC - Agroecology Research Community Garden	49. ELABN - Liberal Arts Building North (SBSC - Social and Behavior Science)	60. ESTHC - Student Health Center
5. EPACA - Performing Arts Complex A (PACA - Fine Arts Building A)	21. EENGR - Engineering	37. EGRNH - Greenhouse	50. EUNTY - Unity Hall	61. EUREC - University Recreation (WRSC - Wellness & Recreation Sports Complex)
6. ESWKH - Southwick Hall	22. EACSB - Academic Services	38. EPOB9-13 - Portable Buildings 9, 10, 11, 12, 13	51. EASFC - Rio Grande Center for Manufacturing	62. EPOB8 - ROTC Storage
7. EPACC - Performing Arts Complex C (PACC - Fine Arts Building C)	23. EPHYS - Physical Science	39. EEDUC - Education Complex	52. EASFC - Police and Parking & Transportation Offices	63. EROTC - ROTC (HRBL - Human Resources Building)
8. EPACB - Performing Arts Complex B (PACB - Fine Arts Building B)	24. EIMFD - Intramural Fields	40. EMAGC - Mathematics & General Classrooms	53. EASFC - Academic Support Facility	64. EBSBL - Baseball Stadium
9. ESSBL - Executive Tower	25. ETROX - Troxel Hall	41. ECCTR - Computer Center (CCTR - New Computer Center)	54. EVLGA - The Village A	65. ESOC - Soccer and Track & Field Complex
10. ESSBL - Student Services Building	26. EHRTG - Heritage Hall	42. ECOBE - Robert C. Vackar College of Business and Entrepreneurship (BUSA - Business Administration Building)	55. EVLGB - The Village B	66. EPOB14 - Physical Science Portable
11. ESSBL - Visitors Center	27. EEMLH - Emilia Schunior Ramirez Hall	43. ECULP - Central Utility Plant	56. EVLBC - The Village C	67. EIEAB - Interdisciplinary Engineering & Academic Studies
12. EMSAC - Mathematics & Science Academy	28. ESRA - Sugar Road Annex (CHUR - Church of Christ)	44. EHABE - Health Affairs Building East (HSHW - Health Science and Human Services East)	57. EVLBD - The Village D	
13. EMASS - Marialice Shary Shivers	29. EHPE1 - Health & Physical Education Complex Fieldhouse	45. EBNSB - Behavioral Neurosciences	58. EVLBE - The Village E	
14. ESTAC - Student Academic Center	30. EPLAN - H.E.B. Planetarium		59. EVLGF - The Village F	
15. EUCTR - University Center	31. ESCNE - Science		60. EEHSB - Environmental Health & Safety (VWOF - Van Week Building)	
16. ECHAP - Chapel	32. ELCTR - The Learning Center (LEAC - Learning Assistance Center)		61. ETHER - Thermal Storage Tank	

NOTE:
Previous Building Names are in RED

